JOURNAL OF MATERIALS SCIENCE 25 (1990) 2532–2538

Effects of nitrogen on hydrogen embrittlement in AISI type 316, 321 and 347 austenitic stainless steels

P. ROZENAK
Materials Engineering Department, Ben-Gurion University of the Negev, Beer-Sheva 84105, Israel

Hydrogen embrittlement of AISI type 316, 321 and 347 stainless steels with nitrogen alloying has been studied by a tensile test through cathodic charging. The results show that addition of nitrogen improved resistance to hydrogen cracking regardless of the failure mode. Fracture surfaces of cathodically charged steels showed intergranular brittle zones on each side of the fracture surfaces. AISI type 316 with nitrogen alloying stainless steel is more resistant to hydrogen embrittlement than AISI type 321 with nitrogen alloying steel, whereas AISI type 347 with nitrogen alloying steel is susceptible to hydrogen embrittlement. Nitrogen alloying of stainless steel increased the mechanical properties in hydrogen environments by increasing the stability of austenite.

1. Introduction

Following early works [1–3], hydrogen embrittlement of austenitic stainless steels has become a well-studied field, and has recently been recognized by other workers [4–11]. Degradation of mechanical properties in hydrogen environments has been attributed, in part, to dislocation motions [3, 5, 12], α'-martensite [13–16], secondary phases [17, 18], surface effects [4, 19] and metallurgical variables [11, 20].

Nitrogen atoms in octahedral sites in the face-centred cubic lattice of a highly alloyed stainless steel produce spherical distortions [21] which are capable of the weak interaction with the edge component of dislocation, although there is no first-order interaction with the screw component. Such interaction would be the cause of the nitrogen strengthening. The effect of nitrogen content on the austenite stability has only a minor effect on stacking fault energy [22, 23], but small changes in nitrogen concentrations of austenitic stainless steels had a strong effect on the M_s [24, 25] and $M_{d_{30}}$ temperatures [26].

The purpose of this study was to evaluate the effect of nitrogen on hydrogen susceptibility of AISI type 316, 321 and 347 austenitic stainless steels. Correlation between the mechanical properties of hydrogen-charged thin specimens with their mode of fracture was also done.

2. Experimental procedure

Commercial austenitic stainless steels of type 316, 321 and 347, having the compositions shown in Table I, were used in this study. The materials were in the form of cold-rolled foils of 0.1 mm thickness. All the samples used in these experiments were solution annealed for 1 h at 1100° C and then quenched in water. Some samples in this group were given nitrogen annealing heat treatment at 1100° C for 1 h. The nitrogen concentration in these steels increased to 0.282, 0.280 and 0.283 wt % in 316, 321 and 347 steels, respectively. Grain sizes, as measured by the method given in ASTM standard E-112 [27], were ASTM 4 in AISI type 316 and 321 stainless steels and ASTM 8 in AISI type 347 stainless steel. Tensile specimens were prepared with their long axes parallel to the rolling direction according to ASTM standard E-8 [28]. The samples were tensile tested at room temperature at an extension rate of $0.005\,cm\,min^{-1}$ while undergoing cathodic charging. The hydrogen charging cell contained 1 N $NaAsO_2$ added as a hydrogen recombination poison. A platinum electrode and a current density of $50\,mA\,cm^{-1}$ were used. The hydrogen content was determined in the Leco hydrogen analyser and was about 1 at % after 24 h cathodic charging at room temperature in vacuum-annealed specimens. Only minor differences in hydrogen concentrations

TABLE I Chemical composition of AISI type 316, 321 and 347 austenitic stainless steels

Element	Amount (wt %) of element in stainless steels		
	AISI 316	AISI 321	AISI 347
N	0.05	0.045	0.048
C	0.05	0.072	0.064
Cr	16.8	17.5	16.3
Ni	13.2	10.7	11.2
Mn	2.07	2.06	2.0
Si	0.41	0.35	0.38
S	0.0015	0.0015	0.0015
P	0.016	0.015	0.015
Mo	2.08	0.2	0.3
Ti	–	0.49	–
Nb	–	–	0.61
Fe	bal.	bal.	bal.

0022–2461/90 $03.00 + .12

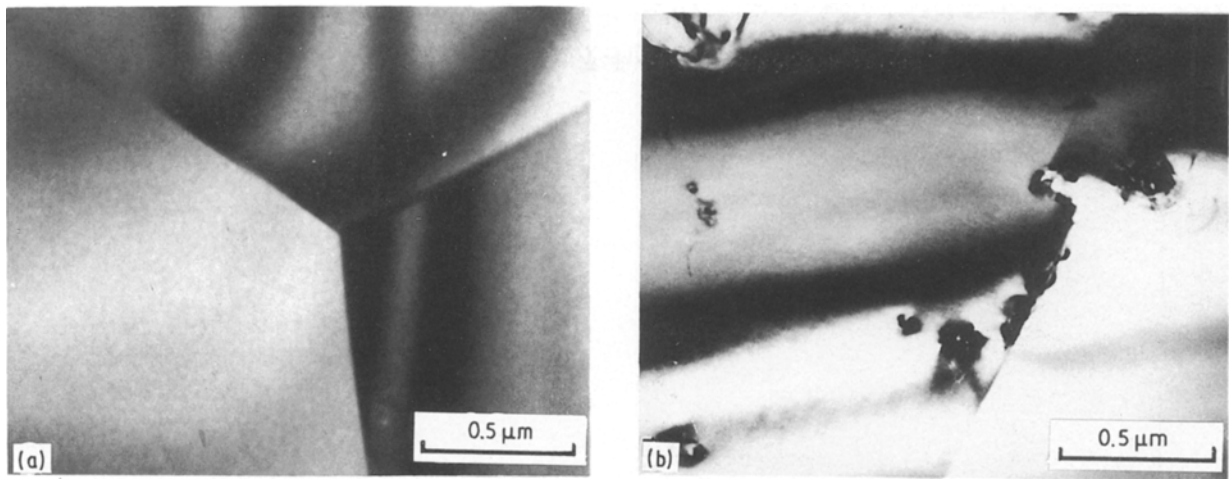

Figure 1 Transmission electron micrographs showing microstructures in the AISI type 316, 321 and 347 stainless steels: (a) austenizing structure in the AISI 316 stainless steel; (b) fine precipitation at carbides within the grains and at grain boundaries in the AISI type 321 stainless steel; (c) precipitation of carbides within the grain in the AISI type 347 stainless steel.

were found in various types of steels and after annealing with nitrogen. After failure, the fracture surfaces were examined with a scanning electron microscope. The microstructures from the various starting conditions were characterized using transmission electron microscopy.

3. Results and discussion

Both vacuum- and nitrogen-annealed heat treatments produced fully austenitic microstructures in AISI type 316 stainless steel (Fig. 1a). Examination of the microstructures of AISI 321 steel revealed grain-boundary Ti(C, N) precipitates and dense distribution of these precipitates within the grains after vacuum- or nitrogen-annealing treatments (Fig. 1b), which varied in size from 10 to 500 nm. Nb(C, N) precipitates were observed on matrix dislocations (Fig. 1c) in both vacuum- and nitrogen-annealed AISI type 347 stainless steels.

The effects of nitrogen on the mechanical properties of AISI type 316, 321 and 347 austenitic stainless steels tested in air (solid lines) are given in Figs 2 to 4. The yield strength and ultimate tensile strengths increased, but the elongation decreased in all kinds of steel. As can be seen from Fig. 2, AISI type 316 steel tested in air, resulted in a 43% reduction of elongation; while the yield and the ultimate tensile strengths increased about 210% and 122%, respectively, with increasing nitrogen content of the steel to a value of 0.28 wt %. The yield strength and ultimate tensile strengths of AISI type 321 steel nitrogenized and tested in air increased about 186% and 66%, respectively, while elongation decreased by 49% (Fig. 3). In AISI type 347 steel the yield and ultimate tensile strengths increased about 175% and 66%, respectively,

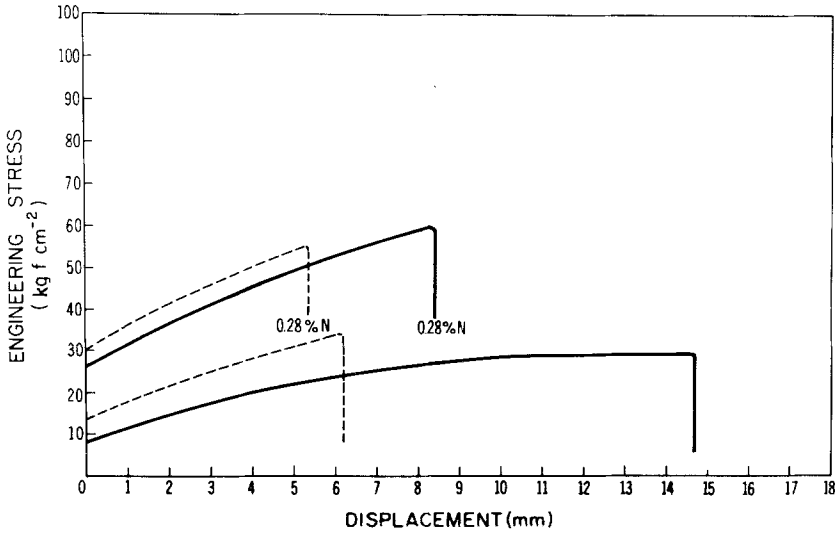

Figure 2 Engineering stress–displacement curves for AISI type 316 stainless steel (vacuum or nitrogen annealed) (——) tensile tested in air and (– – –) undergoing cathodic charging.

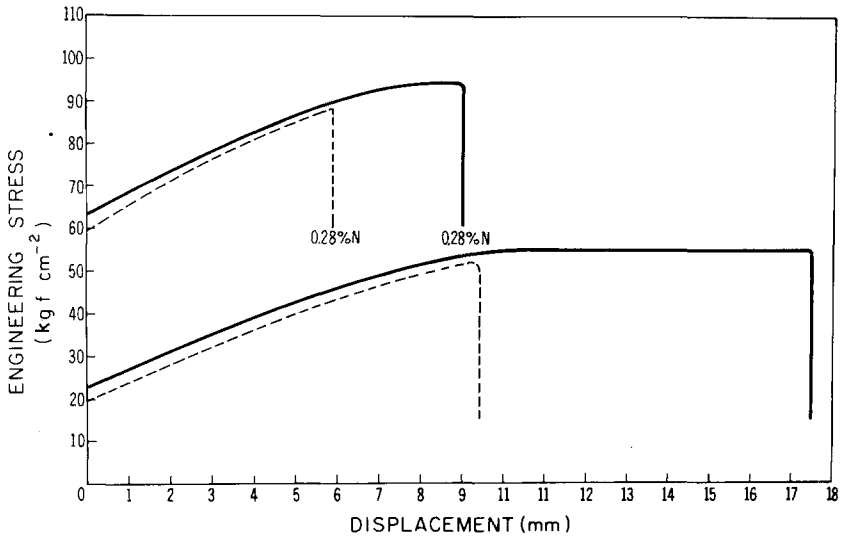

Figure 3 Engineering stress–displacement curves for AISI type 321 stainless steel (vacuum or nitrogen annealed) (——) tensile tested in air and (– – –) undergoing cathodic charging.

while elongation decreased 31% in nitrogen-annealed specimens (Fig. 4).

The influence of the hydrogen on the tensile properties is shown for vacuum- and nitrogen-annealed AISI type 316, 321 and 347 stainless steels (Figs 2 to 4, dashed lines). A significant feature of the results is that an increase of nitrogen content of the steels, increased the mechanical properties (related to properties obtained in air) and the resistance of AISI type 316, 321 and 347 steels to hydrogen embrittlement. The yield strength of the vacuum- and nitrogen-annealed samples under cathodic polarization were increased about 17% and 7%, respectively, compared to the yield strengths of AISI type 316 steel tensile tested in air. There were small differences in AISI type 321 and 347 steels between the yield strengths of cathodically charged, compared to air-tested, steels within the various annealing treatments. Hydrogen has marked effects on ultimate tensile strength and elongation. As can be seen from Fig. 2, vacuum-annealed 316 type cathodically charged specimens showed it to be the most susceptible steel; the reduction of elongation is 58% for cathodically charged compared to air tensile-tested specimens, while nitrogen-annealed specimens resulted in 33% reduction in elongation and 7% reduction in ultimate tensile strength. However, the room-temperature tensile test under cathodic charging resulted in 12% reduction of ultimate tensile strength and 46% reduction in elongation in the vacuum-annealed AISI type 321 steel, while 10% and 36% reduction in ultimate tensile strength and elongation, respectively, were observed in nitrogen-annealed specimens, compared to specimens that were tested in air (Fig.3). AISI type 347 steel showed a 15% reduction in ultimate tensile strength and a 43% reduction in elongation of the vacuum-annealed samples, while the nitrogen-annealed samples showed a reduction of about 12% in ultimate tensile strength and a 39% reduction in elongation under cathodic charging through tensile tests (compared to tensile tested in air specimens). A summary of these results is given in Table II where the yield strength, ultimate tensile strength and elongation of various steels and heat treatments are listed.

After testing, the fracture surface of each specimen was examined to determine the mode of the failure. Ductile dimple rupture with microvoid coalescence was the main fracture mode in both vacuum- and nitrogen-annealed specimens tested in air (Fig. 5). The differences obtained in the fracture surfaces were in the reduction areas of the fracture, which were larger in the vacuum-annealed specimens tested in air. Examination of the sides of the fracture surfaces of these specimens showed typical slip-band structures with

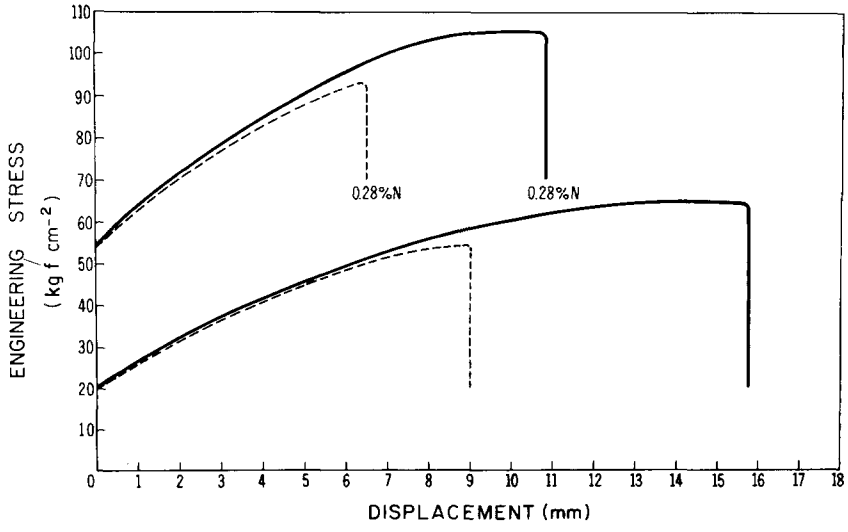

Figure 4 Engineering stress–displacement curves for AISI type 347 stainless steel (vacuum or nitrogen annealed) (——) tensile tested in air and (– – –) undergoing cathodic charging.

TABLE II Percentage reduction (increases) in tensile properties of charged specimens compared with those of uncharged specimens for AISI type 316, 321 and 347 stainless steels

Type of stainless steel	Annealing heat treatment	Reduction (%) in tensile properties		
		Yield	Ultimate tensile strength	Elongation
AISI 316	vacuum	incr. 17	incr. 14	58
AISI 316	nitrogen	incr. 7	7	33
AISI 321	vacuum	10	12	46
AISI 321	nitrogen	10	10	36
AISI 347	vacuum	–	15	43
AISI 347	nitrogen	–	12	39

crystallographic orientations, that are typical of ductile fractures of both vacuum- and nitrogen-annealed specimens (Figs 5b, d).

The fracture surfaces obtained from specimens after tensile tests under cathodic charging show considerable differences. A typical ductile fracture with microvoid coalescence was the main fracture mode in vacuum- and nitrogen-annealed AISI type 316 specimens, which include narrow intergranular zones of about 5 μm on both sides of the fractures (Fig. 6). The same fracture surface was obtained after hydrogen charging of nitrogen-annealed samples, except for slight losses in reduction (Fig. 6c). These changes in the fracture mode were observed in the regions of highest hydrogen concentrations (near the surface) as would be expected if the fracture mode was caused by absorbed hydrogen. The tendency for hydrogen-induced surface cracking in the necked area obtained in vacuum- and nitrogen-annealed AISI type 316 specimens (Fig. 6b). The mode of surface cracking was intergranular with secondary transgranular cracks.

The main fracture mode for nitrogen-annealed AISI type 321 stainless steel was a typical brittle transgranular fracture, while intergranular narrow zones of about 5 μm were observed on both outer surfaces of the samples (Fig. 7). Examination of the sides of the fracture surface of AISI type 321 steel showed intergranular main cracks with secondary intergranular

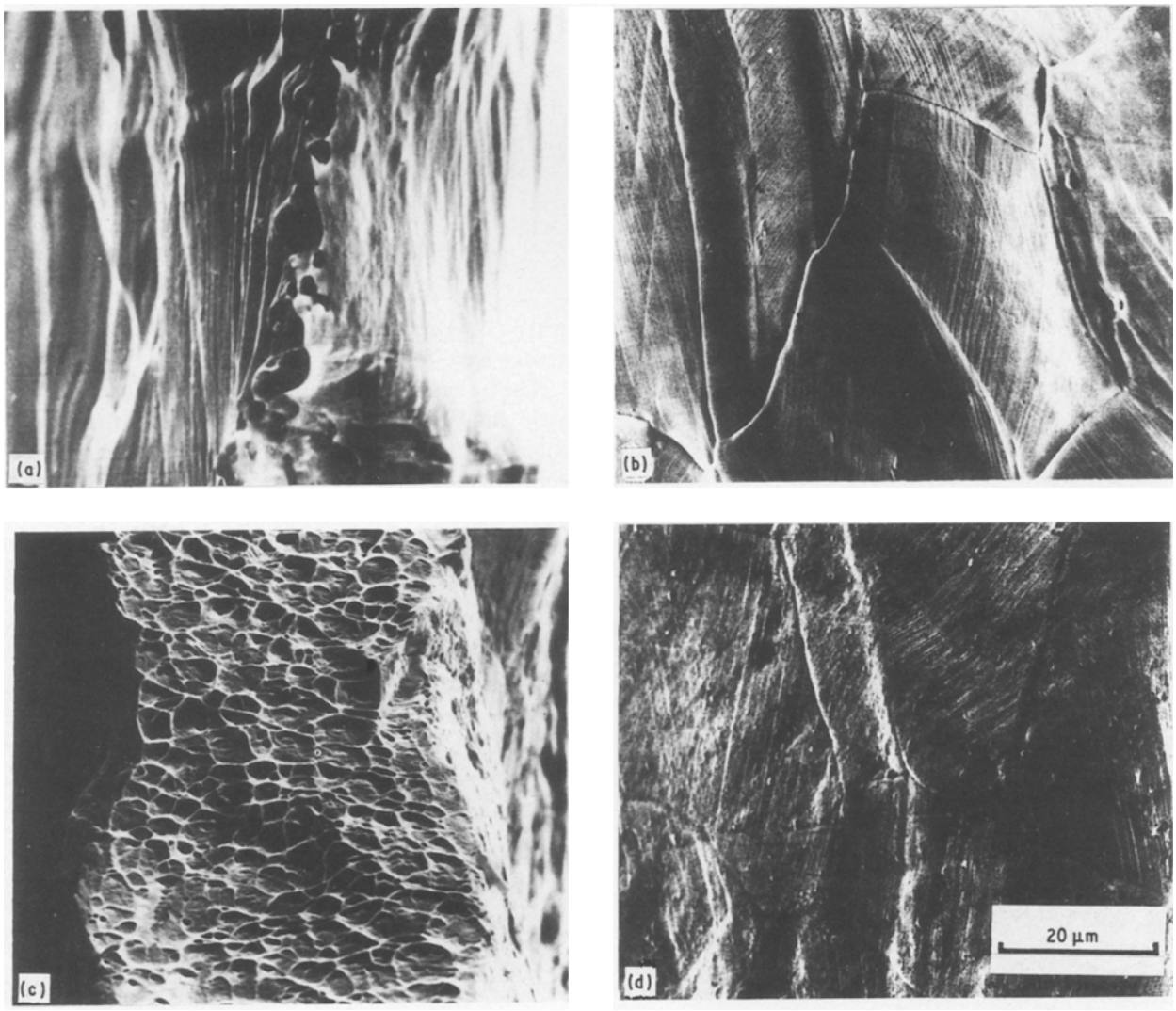

Figure 5 Micrographs of (a), (c) the fracture surface, and (b), (d) the side of the fracture surface of AISI type 316 stainless steel tensile tested in air: (a), (b) annealed; (c), (d) nitrogenized.

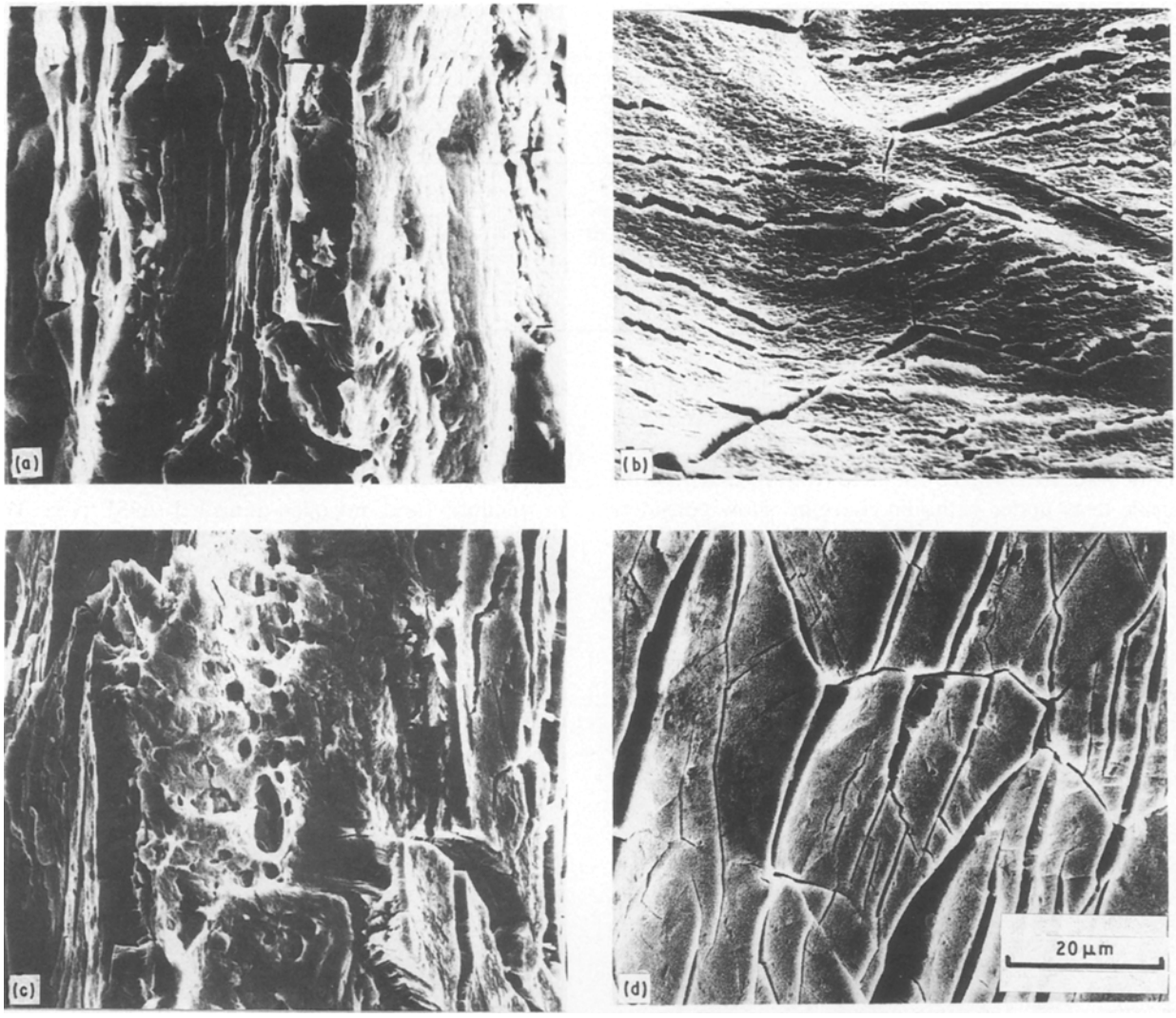

Figure 6 Micrographs of (a), (c) the fracture surface, and (b), (d) the side of the fracture surface of AISI type 316 stainless steel tensile tested while undergoing cathodic charging: (a), (b) annealed; (c), (d) nitrogenized.

cracks (Fig. 7b). The main fracture mode of nitrogen-annealed AISI type 347 steel was a typical transgranular ductile fracture, while intergranular brittle narrow (5 μm wide) zones on two sides of the fracture surfaces were observed (Fig. 8). Coalescence of voids and formation of chains of voids were observed between the brittle–ductile zones (Fig. 8a). Surface cracking typical of hydrogen-charged samples developed in both vacuum- and nitrogen-annealed samples, when intergranular and transgranular secondary cracks were obtained (Fig. 8b).

The interstitial solute-like nitrogen increases the yield strength [21, 29] and its effects seem to be linear function of concentration [21]. Nitrogen in the solid solution influences the lattice parameter of the austenite, and thus strain is introduced into the lattice which induces solid solution strengthening effects. Nitrogen is a strong austenite stabilizer [24–26]. The formulae

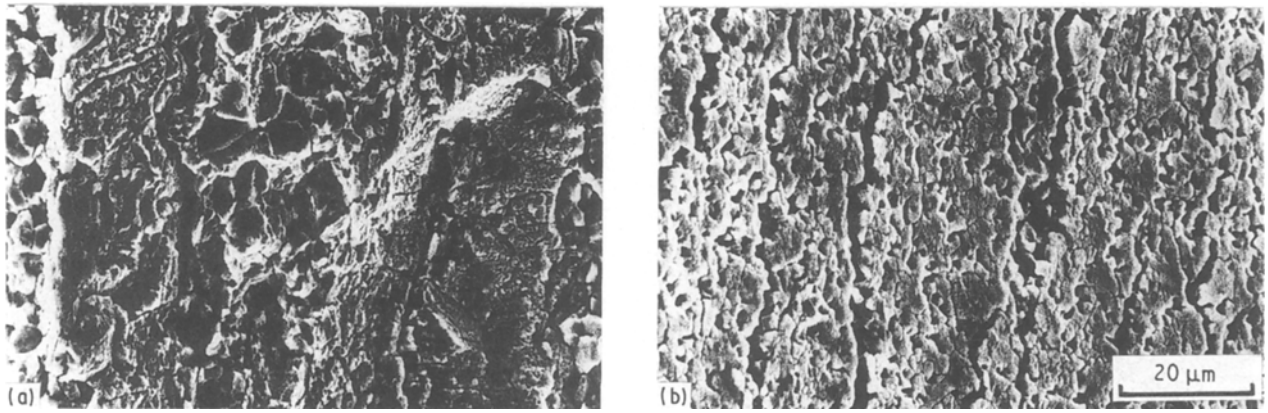

Figure 7 Micrographs of (a) the fracture surface, and (b) the side of the fracture surface of AISI type 321 stainless steel nitrogenized and tensile tested while undergoing cathodic charging.

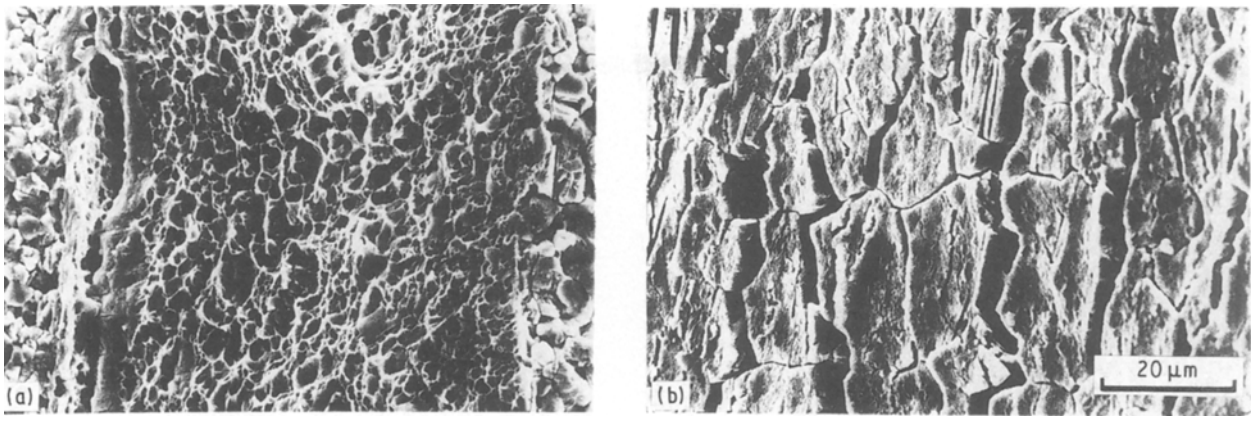

Figure 8 Micrographs of (a) the fracture surface, and (b) the side of the fracture surface of AISI type 347 stainless steel nitrogenized and tensile tested while undergoing cathodic charging.

for stability of austenite given by M_s and/or $M_{d_{30}}$ temperatures are [24, 26]

$$M_s(^\circ C) = 1305 - (61Ni) - (41.7Cr) - (33.3Mn) - (27.8Si) - [1667(C + N)] \quad (1)$$

$$M_{d_{30}}(^\circ C) = 413 - 462(C + N) - 9.2(Si) + 8.1(Mn) - 13.7(Cr) - 9.5(Ni) - 18.5(Mo) \quad (2)$$

However, martensite can be produced during straining in the tensile test. Martensite formation from the austenite is important, largely due to its effect on ductility, but it also influences its strength [25]. Strength relationships obtained between nitrogen in solid solution and the yield and the tensile strengths (Figs 2 to 4), have been reviewed recently by others [21, 25, 30].

Hydrogen concentration on the sample surfaces during cathodic charging corresponds to approximately one hydrogen atom per matrix atom, due to the fact that cathodic charging is equivalent to gaseous charging at extremely high hydrogen fugacities (≈ 10 atm) [31]. The small lattice diffusivity of hydrogen in austenite ($D \approx 8 \times 10^{-16}$ m^2 sec^{-1} at 300 K) [32], coupled with its high fugacity, was responsible for the attachment of the high surface concentration gradients beneath the surface. Atrens *et al.* [31], who calculated the concentration profiles resulting from hydrogen charging of austenite, have shown that immediately after charging, the hydrogen concentration falls by a factor of 10 within the first 5 μm of the surface. No significant effect of plastic deformation on hydrogen diffusivity was observed for the stable 310 stainless steel [33]; in the 304 stainless steel, an increased deep of diffusion profiles to results from plastic deformation which could be attributed to deformation induced α'-martensite formation. In fact the hydrogen concentration is non-uniform within the grains of the microstructure near the surface regions of the charged samples. Non-uniform concentrations of hydrogen result in non-uniform expansion, which in turn leads to the development of internal stresses [34, 35]. The existence of two narrow intergranular zones (Figs 6 to 8), one on each side of the fracture surface of the vacuum- and nitrogen-annealed AISI types 316, 321 and 347 stainless steels and intergranular and secondary transgranular cracking of the surface fractures sides, is probably due to the interaction of the outer surfaces, where high hydrogen fugacities under the applied stresses were observed. Microvoid coalescence producing ductile rupture in the middle of the specimens was typical of regions not affected by hydrogen (Figs 5, 6 and 8). Several workers have reported that fracture of specimens which showed induced ductility losses was completely ductile, and that the presence of hydrogen reduced the size of the dimples, which is typical of ductile fractures [3, 8, 36]. A dense distribution of M(C, N) precipitates within the grains on the matrix dislocations, thereby promoting the transgranular fracture of AISI type 321 stainless steel (Fig. 7). Hydrogen might be influential due to alloying effects, to alteration of transformation temperatures (M_s or M_d), or to its effect on the stacking fault energy (SFE). Internal stresses or strain, which accompany the absorption of the supersaturated hydrogen, might provide a significant driving force for austenite decomposition. Particular changes occurring in the M_s and $M_{d_{30}}$ temperatures range should be considered, because metastable austenite can be activated by an external or an internal stress field [37]. The principal effect of hydrogen was to decrease the stress required for phase transformations of austenite [35], and the γ-phase can transform to ε- or α'-martensites, which may be induced, at lower stresses [38]. Many workers [16–19, 39, 40] have suggested that the presence of deformations and hydrogen-induced martensite greatly increase the susceptibility of austenitic stainless steel to hydrogen cracking. The measured hydrogen contents show that addition of nitrogen has no marked effect on hydrogen solubility in the austenite during the charging. Therefore, the improved resistance of AISI type 316, 321 and 347 austenitic stainless steels to hydrogen embrittlement by nitrogen addition (Figs 2 to 4 and Table II) is due to the increasing stability of austenite.

4. Conclusions

1. Addition of nitrogen to a solid solution of austenite in AISI type 316, 321 and 347 stainless steels improves their resistance to hydrogen embrittlement.

2. Fracture surfaces of vacuum- and nitrogen-

annealed specimens tested through cathodic charging showed massive regions of microvoid coalescence or transgranular fracture, producing rupture with two narrow intergranular zones, one on each side of the fracture surface of the austenitic stainless steels.

3. AISI type 347 with nitrogen alloying stainless steel is more susceptible to hydrogen embrittlement than is AISI type 321 with nitrogen alloying steel, and AISI type 316 with nitrogen alloying is the most resistant steel in hydrogen environments.

Acknowledgements

The author wishes to acknowledge Mr B. Latipov (Ben-Gurion University) for technical assistance.

References

1. M. L. HOLZWORTH, *Corrosion* **26** (1969) 107.
2. M. B. WHITEMAN and A. R. TROIANO, *ibid.* **21** (1965) 53.
3. M. R. LOUTHAN Jr, G. R. CASKEY Jr, J. A. DONOVAN and D. E. RAWL Jr, *Mater. Sci. Engng* **10** (1972) 357.
4. M. R. LOUTHAN Jr, in "Hydrogen in Metals", edited by I. M. Bernstein and A. W. Thompson (American Society for Metals, Metals Park, Ohio, 1974) p. 53.
5. A. W. THOMPSON, *ibid.*, p. 91.
6. A. J. WEST and M. R. LOUTHAN Jr, *Met. Trans.* **13A** (1982) 2049.
7. A. W. THOMPSON, in "Environmental Degradation of Engineering Materials", edited by M. R. Louthan Jr, and R. P. McNitt (Printing Department, Virginia Polytechnic Institute, Blacksburg, Virginia, 1977) p. 3.
8. A. W. THOMPSON and J. A. BROOKS, *Metall. Trans.* **A6** (1975) 1931.
9. C. L. BRIANT, in "Proceedings of the International Conference on Hydrogen Effects in Metals", Moran, 1980, edited by I. M. Bernstein and A. W. Thompson (Metallurgical Society of AIME, Warrendale, Pennsylvania 1980) p.527.
10. H. HANNINEN, T. HAKKARAINEN and P. NENONEN, *ibid.*, p. 575.
11. P. ROZENAK and D. ELIEZER, *Mater. Sci. Engng* **61** (1983) 31.
12. C. HWANG and I. M. BERNSTEIN, *Acta Metall.* **34** (1986) 1001.
13. M. L. HOLZWORTH and H. R. LOUTHAN Jr, *Corrosion* **24** (1968) 110.
14. R. LIU, N. NARITA, C. ALTSTETTER, H. BIRNBAUM and N. PUGH, *Metal. Trans.* **11A** (1980) 1563.
15. W. Y. CHU, J. YAO and C. M. HSIAO, *ibid.* **15A** (1984) 729.
16. D. ELIEZER, G. CHAKRAPANI, C. J. ALTSTETTER and E. PUGH, *ibid.* **10A** (1979) 935.
17. C. L. BRIANT, *ibid.* **10A** (1979) 181.
18. A. W. THOMPSON, *Mater. Sci. Engng* **14** (1974) 253.
19. R. M. VENNET and G. S. ANSELL, *Trans. ASM* **60** (1967) 242.
20. Y. ROSENTAL, M. MARC-MARKOWITCH and A. STERN, *Scripta Metall.* **15** (1989) 861.
21. H. L. G. BYRNES, M. GRUJICIC and W. S. OWEN, *Acta Metall.* **35** (1987) 1853.
22. C. G. RHODES and A. W. THOMPSON, *Metal. Trans.* **89A** (1977) 1901.
23. P. Q. SWANN, *Corrosion* **19** (1963) 102.
24. G. H. EICHELMAN and F. C. HULL, *Trans. ASM* **45** (1953) 77.
25. F. B. PICKERING, in "Optimization of Processing, Properties and Service Performance through Microstructural Control", edited by H. Abrams, G. N. Maniar, D. A. Nail and H. D. Solomon (American Society for Testing and Materials, Philadelphia, 1979) p. 263.
26. T. ANGEL, *J. Iron Steel Inst.* **177** (1954) 165.
27. ASTM Standard E-112, (American Institute for Testing and Materials, Philadelphia, Pennsylvania, 1977).
28. ASTM Standard E-8, *ibid.* (1976).
29. K. J. IRVINE, T. GLADMAN and F. B. PICKERING, *J. Iron Steel Inst.* **207** (1969) 1017.
30. K. J. IRVINE, D. T. LEEWELLYN and F. B. PICKERING, *ibid.* **199** (1961) 153.
31. A. ATRENS, J. BELLIMA, N. FIORE and R. COYE, in "The Metal Science of Stainless Steel", edited by E. Collings and H. Kings (American Institute of Mechanical Engineers, New York, 1979) p. 54.
32. P. STUDEBAKER, C. ALSTETTER and W. CONLEY, in "Effects in Metals", edited by I. M. Bernstein and A. W. Thompson (American Institute of Mechanical Engineers, Warrendale, Pennsylvania, 1981) p. 169.
33. B. LADNA and H. K. BIRNBAUM, *Acta Metall.* **35** (1987) 1775.
34. P. ROZENAK, L. ZEVIN and D. ELIEZER, *J. Mater. Sci. Lett.* **2** (1983) 63.
35. P. ROZENAK and D. ELIEZER, *Acta Metall.* **35** (1987) 2329.
36. A. W. THOMPSON, *Metall. Trans.* **10A** (1979) 731.
37. H. MATHIAS, Y. KATZ and S. NADIV, *Metal Sci.* **12** (1978) 129.
38. P. ROZENAK, I. M. ROBERTSON and H. K. BIRNBAUM, *Acta Metall.*, in press.
39. R. B. BENSON, R. K. DANN and L. W. ROBERTS Jr, *Trans. Met. Soc. AIME* **242** (1968) 2199.
40. C. L. BRIANT, *Scripta Metall.* **12** (1978) 541.

Received 20 March
and accepted 4 September 1989